Pressure broadening and shift of He($2\ ^3P_{0,1,2}$)-He($2\ ^3S$) lines

D. Vrinceanu, S. Kotochigova,* and H. R. Sadeghpour
ITAMP, Harvard-Smithsonian Center for Astrophysics, Cambridge, Massachusetts 02138, USA
(Received 23 September 2003; published 26 February 2004)

The collisional broadening and shift of metastable helium fine-structure lines are calculated within the impact approximation. *Ab initio* Born-Oppenheimer potential energy curves correlating to He($1\ ^1S_0$) and He($2\ ^3P_j$) atomic levels are obtained using the configuration interaction valence bond method and combined with semiempirically calculated van der Waals interaction terms between these atoms to also study *j*-specific and *j*-changing collisions. A long-range van der Waals potential well exists in the $^3\Pi_u$ potential correlated to the He($1\ ^1S_0$)+He($2\ ^3P_j$) limit, whose influence on the scattering phase shift is assessed. At $T=310$ K, the broadening and shift parameters are practically *j* independent and have average values of 12.60 and 1.87 MHz/Torr, respectively. The *j*-changing collisions have cross sections roughly five times smaller than the *j*-specific cross sections.

DOI: 10.1103/PhysRevA.69.022714 PACS number(s): 34.20.Cf, 31.15.Rh, 33.70.Jg

I. INTRODUCTION

Radiation damping of an excited atom leads to a broadening of spectral lines. Such broadening or natural broadening is often modified in the presence of collisions with background atoms in a gas or in a plasma. There is also a shift of spectral lines associated with collisions. The collisional broadening and shift of lines are critical for precision spectroscopy and can be used as temperature diagnostics of electron or ion densities in a gas [1].

Careful analysis of line profiles is a powerful technique for studying atomic and molecular interactions and is often necessary for probing matter in extreme conditions, such as in stellar atmospheres, ultracold traps, liquid helium, and Bose-Einstein condensates. Broadening of spectral lines of implanted atoms in superfluid helium or clusters has been used to probe cavity structure and bubble evolution in liquids [2]. The radiative scattering process can also be employed to investigate the nature of interatomic interactions [3,4].

There is a considerable literature (e.g., [5,6]) on the study of line broadening processes. The impact approximation, originally due to Baranger [7], has been widely and successfully used for treating the pressure broadening and shift of lines. This approximation assumes that (a) the spectral lines are well separated, (b) only binary collisions are important for the broadening and shift of lines, and (c) the collision time is much less than the time between collisions. The impact approximation is particularly suited to the line core and gives a Lorentzian profile for the line intensity,

$$I(\omega)\sim \frac{|\langle\beta|e\mathbf{r}|\alpha\rangle|^2}{(\omega-\omega_0-d)^2+(\Gamma/2+w)^2}, \qquad (1)$$

where Γ is the natural width of the spectral line and the numerator is the square of the dipole amplitude for a free-free transition between initial ($|\alpha\rangle$) and final ($|\beta\rangle$) states of the radiator-perturber system. The laser frequency ω is tuned with respect to the unperturbed transition frequency ω_0, and the broadening width w (half width at half maximum) and shift *d* are given as averages over all collisions of the corresponding transition rates.

Far from the line core, in the wings of the transition profile, the impact approximation fails. The quasistatic approximation [6], based on the slow relative motion of the radiator-perturber system, results in an intensity distribution that depends on the difference of the interaction between the perturbing and radiating atoms in the ground and excited states. For a purely van der Waals interaction (C_6/R^6) between the radiator and perturber, the intensity varies as $I(\omega)\propto\delta^{-3/2}$, where $\delta=\omega-\omega_0$ is the detuning. This behavior was first observed by Kuhn [8] for the red wing of a mercury line at 253.7 nm, perturbed by argon.

The quasimolecular model of optical collisions deals with line profiles within the framework of the adiabatic two-channel approximation for the interaction of a perturber with a radiating atom in its initial and excited states. Such a treatment has been coined the unified Franck-Condon (UFC) theory for the absorption profile [5] and has been extended to the study of broadening where nonadiabatic effects, such as the Coriolis coupling of Σ-Π symmetries, occur [4]. Julienne and Mies showed that the UFC approximation is obtained by simply making the linewidth w in Eq. (1) dependent on the detuning δ; the impact approximation is obtained in the limit $\delta\rightarrow 0$.

The present work deals with on-resonance Doppler-free saturation laser spectroscopy of helium transitions He($^3S_1$-$^3P_{0,1,2}$) under the influence of collisions with He($1\ ^1S_0$) atoms [9]. The fine-structure splitting of the He($2\ ^3P_j$) levels in helium have been exploited in various experiments [10–13] to measure the fine-structure constant α and for quantitative tests of QED. Because the experimental number ratio of metastable to normal helium atoms is very small [13], only the pressure broadening and shift of levels resulting from collisions between the ground He($1\ ^1S_0$) atoms with He($2\ ^3S_1$) and He($2\ ^3P_j$) metastable atoms need to be considered. To this end, we calculate *ab initio* molecular potentials for the ground and excited dimer

*Present address: National Institute of Standards and Technology, Gaithersburg, MD 20899, USA.

states, correlating to $^1S+{}^3S$ and $^1S+{}^3P$ limits.

Elastic scattering phase shifts in all optically coupled molecular potentials are calculated and then transformed from the rotating molecular frame, or body-fixed (BF) frame, to the atomic-fixed frame, or space-fixed (SF) frame, where the individual atomic total angular momenta j_1 and j_2 are good quantum numbers. This transformation is in spirit similar to the frame transformation ideas put forth by Fano [14] and Arthurs and Dalgarno [15]. The frame transformation techniques for diatomic molecules and the angular momentum dependence of cross sections have been studied by Singer *et al.* [16], Pack and Hirschfelder [17], Reid and Rankin [18], Leo *et al.* [19], and more recently by Krems and Dalgarno [20]. Line shift and broadening parameters and elastic and *j*-changing cross sections are calculated for different fine-structure transitions and compared with measurements [21]. In this approach, rotational coupling is implicitly included; the Hamiltonian is solved in the uncoupled representation in the BF frame. The transformation to the SF frame brings in the necessary coupling. For room temperature such an approximation is sufficient.

II. THEORETICAL FRAMEWORK

A. Impact approximation

Although the radiating or absorbing atom is generally embedded in a perturber bath and the collision process is a large many-body problem, the quantum mechanical treatment of the collision begins with a single binary collision between the perturber and perturbed atom. The interaction between perturbing atoms is ignored and each perturber interacts *only* with one perturbed atom at a time. In the impact approximation [7,22], the shift and broadening parameters are *linearly* proportional to the perturber density and depend on the perturber-radiator interaction only through the scattering phase shift or matrix elements for binary collisions before and after absorption or emission. These parameters can also be related to the spectral profile of free-free transitions for the perturber-radiator diatom, as illustrated in Fig. 1.

The spectral line profile for transitions from the initial states $|j_\alpha m_\alpha\rangle$ to the final states $|j_\beta m_\beta\rangle$ in collision with a perturber atom is

$$\Delta \equiv \mathrm{w} - id = \frac{\hbar^2 \pi n}{\mu^2} \int_0^\infty \frac{f(v)}{v} dv \, \frac{1}{(2j_\alpha+1)} \times \sum_{\text{all } m's} \sum_{\ell\ell'} C^{j_\beta m_\beta}_{j_\alpha m_\alpha, 1q} C^{j_\beta m_\beta}_{j_\alpha m'_\alpha, 1q} [\delta_{m_\alpha m'_\alpha} \delta_{m_\alpha m'_\alpha} \delta_{\ell\ell'} - S^{(\alpha)}_{j_\alpha m_\alpha \ell m \to j_\alpha m'_\alpha \ell' m'} S^{*(\beta)}_{j_\beta m_\beta \ell m \to j_\beta m'_\beta \ell' m'}], \quad (2)$$

where n is the perturber density, $|jm\rangle$ and $|jm'\rangle$ refer to the atomic total angular momentum and their projections on the SF axis of the radiating atom, ℓ, m and ℓ', m' are the relative perturbed-perturber orbital angular momentum quantum numbers, and $C^{j_\beta m_\beta}_{j_\alpha m_\alpha, 1q}$ are the Clebsch-Gordan coefficients ($C^{jm}_{j_1 m_1 j_2 m_2} = \langle j_1 m_1, j_2 m_2 | jm \rangle$) coupling the initial and final states via a photon of polarization, $\hat{\epsilon}_q$. The primes refer to states immediately after the collision and all m values are defined with respect to the SF frame. An average over the relative perturber-radiator Maxwell-Boltzmann velocity distribution,

$$f(v) = 4\pi v^2 \left(\frac{\mu}{2\pi k_B T}\right)^{3/2} \exp\left(-\frac{\mu v^2}{2k_B T}\right),$$

at a temperature T, is taken [19,23]. If the Zeeman levels are not resolved, the expression for the width and shift becomes [24]

$$\mathrm{w} - id = \frac{\hbar^2 \pi n}{\mu^2} \int_0^\infty \frac{f(v)}{v} dv \sum_{JJ',\ell\ell'} (2J_\alpha+1)(2J_\beta+1) \times (-1)^{l+l'} \begin{Bmatrix} J_\beta & J_\alpha & 1 \\ j_\alpha & j_\beta & \ell \end{Bmatrix} \begin{Bmatrix} J_\beta & J_\alpha & 1 \\ j_\alpha & j_\beta & \ell' \end{Bmatrix} \times [\delta_{\ell\ell'} - S^{(J_\alpha)}_{j_\alpha \ell \to j_\alpha \ell'}(v) S^{*(J_\beta)}_{j_\beta \ell \to j_\beta \ell'}(v)], \quad (3)$$

where $\mathbf{J} = \boldsymbol{\ell} + \mathbf{j}$ is the total angular momentum of the system in the SF frame and $\{^{abc}_{dfg}\}$ are the usual $6j$ symbols. The scattering matrix elements in the initial (α) and final (β) radiative states are denoted by $S^{(J_\alpha)}$ and $S^{(J_\beta)}$, respectively, and the reduced mass is μ.

The shift and broadening expressions can be rewritten as

$$\mathrm{w} - id \equiv \Delta_{\beta\alpha} = \hbar n \langle v \sigma_{\beta\alpha} \rangle = p \frac{\hbar \langle v \rangle}{k_B T} \langle \sigma_{\beta\alpha} \rangle, \quad (4)$$

where the average velocity is $\langle v \rangle = \sqrt{8 k_B T / \pi \mu}$ and the pressure of the perturber gas is p. The energy averaged cross section is

$$\langle \sigma_{\beta\alpha} \rangle = \int_0^\infty \frac{\epsilon}{k_B T} \sigma_{\beta\alpha}(\epsilon) e^{-\epsilon/k_B T} d\left(\frac{\epsilon}{k_B T}\right),$$

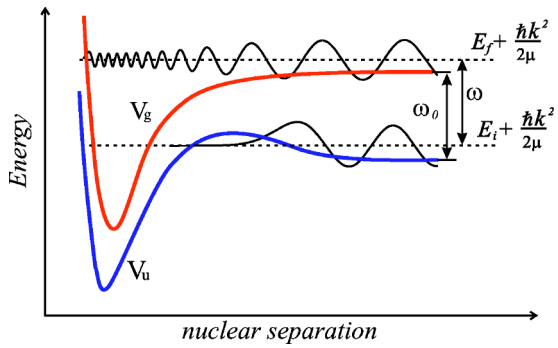

FIG. 1. (Color online) Schematic diagram of the scattering processes involved in the interaction of radiating and perturber atoms. The V_i and V_f are interaction potentials as a function of nuclear separation R for the initial and final states, respectively. Also shown are the scattering solutions for V_i and V_f at a collisional energy of $\hbar^2 k^2/2\mu$, at large internuclear separations. The spectral line shift and broadening are expressed in terms of these solutions.

while energy $\epsilon=\hbar^2k^2/2\mu=\mu v^2/2$ is the same for both initial and final states. Finally, the broadening-shift cross section is defined by

$$\sigma_{\beta\alpha}=\frac{\pi}{k^2}\sum_{J_\alpha J_\beta,\ell,\ell'}[J_\alpha J_\beta]^2\begin{Bmatrix}J_\beta & J_\alpha & 1\\ j_\alpha & j_\beta & \ell\end{Bmatrix}\begin{Bmatrix}J_\beta & J_\alpha & 1\\ j_\alpha & j_\beta & \ell'\end{Bmatrix}\times[\delta_{\ell\ell'}-S^{(J_\alpha)}_{j_\alpha\ell\to j_\alpha\ell'}(v)S^{(J_\beta)\,*}_{j_\beta\ell\to j_\beta\ell'}(v)], \tag{5}$$

with notation: $[XY\cdots]=\sqrt{(2X+1)(2Y+1)}\cdots$.

B. Frame transformation

The scattering matrix elements $S^{(J)}_{j\ell\to j'\ell'}=\langle(j_1j_2)j'\ell',JM|S|(j_1j_2)j\ell,JM\rangle$ are defined in a basis of properly symmetrized SF wave functions

$$\Psi^{JM}_{(j_1j_2)j\ell}(\hat{R},\mathbf{r})=\frac{1}{\sqrt{2}}\sum_{m,n}C^{JM}_{\ell njm}Y_{\ell n}(\hat{R})[\varphi^{(j_1j_2)}_{jm}(\mathbf{r})+p_{AB}(-1)^{j_1+j_2-j+\ell}\varphi^{(j_2j_1)}_{jm}(\mathbf{r})], \tag{6}$$

where $\hat{R}$ is along the internuclear axis and $\mathbf{r}$ stands for the full set electronic coordinates. The electronic wave functions at $R\to\infty$, φ_{jm}, are symmetrized with respect to electron exchange. The quantum number p_{AB} is the eigenvalue of the nuclear permutation operator and is $+1$ for bosonic nuclei and -1 for fermionic nuclei. The appendix gives the procedure for constructing the symmetrized wave functions in both SF and BF frames.

In the limit of large nuclear separation, the symmetrized BF electronic wave functions are (see the Appendix)

$$\Psi^{JM}_{w\Lambda\mu}(\hat{R};\mathbf{r})=\sqrt{\frac{2J+1}{8\pi}}D^{(J)}_{M\Omega}{}^*(\phi,\theta,0)[\varphi^{(\Lambda_1\Lambda_2)}_{\Lambda\mu}(\mathbf{r}')+ww_1w_2\varphi^{(\Lambda_2\Lambda_1)}_{\Lambda\mu}(\mathbf{r}')], \tag{7}$$

where $w=\pm1$ is the gerade-ungerade symmetry quantum number of the homonuclear molecule, w_1 and w_2 are the atomic parities, Λ is the projection of the total orbital angular momentum on the internuclear axis, and μ is the projection of the total spin. A succinct description of the electronic states is $|w(S_1S_2)S\mu(L_1L_2)L\Lambda\rangle\equiv|cw\Lambda\mu\rangle$, where c is a label for all quantum numbers not explicitly listed. For example, the molecular state $He_2(b^3\Pi_g)$ is described by six degenerated states $|b;w=+1,\Lambda=\pm1,\mu=-1,0,1\rangle$. The Wigner matrix $D^{(J)}_{M\Omega}(\phi,\theta,0)$ is defined with respect to the projection quantum numbers $\Omega=\Lambda+\mu$ along the internuclear axis and M along the SF axis.

The R-independent transformation between the wave functions (6) and (7) is obtained from the scalar product $\langle\Psi^{JM}_{(j_1j_2)j\ell}|\Psi^{J'M'}_{cw\Lambda\mu}\rangle\equiv\langle j\ell|w\Lambda\mu\rangle_J\delta_{JJ'}\delta_{MM'}$. From the four basic terms into which this scalar product decomposes, only two are nonzero due to orthogonality of the atomic wave functions, such that

$$\langle j\ell|w\Lambda\mu\rangle_J\equiv\langle(j_1j_2)j\ell JM|w(S_1S_2)S\mu(L_1L_2)L\Lambda J\Omega M\rangle=\frac{1+ww_1w_2(-1)^\ell}{2}\sum_L\begin{bmatrix}j_1 & j_2 & L & S & \ell\\ & & & & J\end{bmatrix}\times C^{J\Omega}_{\ell0j\Omega}C^{j\Omega}_{L\Lambda S\mu}\begin{Bmatrix}j & j_1 & j_2\\ S & S_1 & S_2\\ L & L_1 & L_2\end{Bmatrix}. \tag{8}$$

The desired SF scattering matrix elements can now be related to the calculated BF matrix elements by

$$S^{(J)}_{j\ell'\to j\ell}=\langle j\ell'|S|j\ell\rangle=\sum_{\substack{w\Lambda\mu\\ w'\Lambda'\mu'}}\langle j\ell'|w'\Lambda'\mu'\rangle\langle w'\Lambda'\mu'|S|w\Lambda\mu\rangle\times\langle w\Lambda\mu|j\ell\rangle. \tag{9}$$

Within the range of energies considered here, the S-matrix in the BF frame is diagonal. This is justified in the Born-Oppenheimer picture as long as the spin-orbit couplings are small compared with the electrostatic interaction. At large R, however, the couplings cannot be ignored; the spin-orbit interaction becomes comparable to or dominates over the electrostatic interaction between the atoms and the problem is best solved in the atomic basis. The transformation from the BF to the SF frames accomplishes this task and it permits us to properly apply the boundary conditions and construct the scattering wave functions. We assume a constant asymptotic spin-orbit interaction energy—i.e., the atomic spin-orbit interaction—so that the energy levels are shifted according to the strength of this coupling. The S-matrix elements in the BF frame are

$$\langle w'\Lambda'\mu'|S|w\Lambda\mu\rangle_J=e^{2i\eta^J_{w|\Lambda|}}\delta_{ww'}\delta_{\Lambda\Lambda'}\delta_{\mu\mu'},$$

where $\eta^J_{w|\Lambda|}$ is the Jth partial-wave elastic phase shift in the molecular channel labeled by $w|\Lambda|$. The present approach differs from other calculations that solve a system of coupled Schrödinger equations in terms of the SF wave functions employing the interaction potentials in the BF frame.

III. GROUND-STATE–METASTABLE-STATE HELIUM COLLISION

Our calculation is motivated by a recent experiment in Gabrielse's group at Harvard [13,21] in which the aim is to measure the fine-structure constant through saturated absorption spectroscopy of the spin-orbit levels in the transitions $He(2\,^3S_1-2\,^3P_{0,1,2})$ in a variable-pressure helium vapor cell. The metastable He atoms are produced in an electrical discharge and Doppler-free spectroscopy is achieved by absorbing from two counterpropagating 1083-nm diode laser beams. The lines are affected by the background gas of normal helium atoms at a temperature of about 310 K and are linearly broadened and shifted from their vacuum positions. By extrapolating to zero pressure, the collision-free line intervals can be extracted from the measurements.

States		L	S	w	j
Perturber	He(1^1S_0)	0	0	+1	0
Emitter lower (initial) states	He(2^3S_1)	0	1	+1	1
Emitter upper (final) state	He($2^3P_{0,1,2}$)	1	1	-1	2,1,0

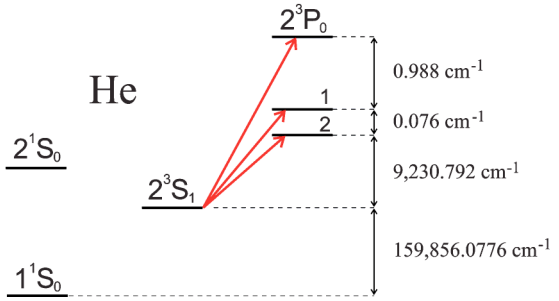

FIG. 2. (Color online) Atomic states of metastable helium involved in the broadening and shift. L and S are the total electronic orbital and spin angular momenta; j is the total angular momentum and w is the parity.

In this work, we treat the collision between the He($1\ ^1S_0$) and He($2\ ^3S_1$, $2\ ^3P_{0,1,2}$) atoms in the Born-Oppenheimer (BO) picture and account for non-BO effects by a frame transformation. This method also allows us to obtain both j-specific and j-changing collision cross sections, whose scattering amplitudes are employed in obtaining shift and broadening parameters. In what follows, the perturber is a He($1\ ^1S_0$) atom and the perturbed or absorber atoms are He($2\ ^3S_1$) in the initial state and He($2\ ^3P_{0,1,2}$) in the final states. A summary of atomic energy levels and the quantum numbers for the perturber and perturbed atoms is presented in Fig. 2.

The lower metastable state He($2\ ^3S_1$) is long lived ($\approx$8000 s), while the upper P states have much shorter lifetimes $\approx$100 ns, so that the natural linewidth of the transition is determined by the excited-state lifetimes, $\Gamma \approx 1.6$ MHz.

A. Molecular potentials

The interaction in the initial channel [He($1\ ^1S_0$)+He($2\ ^3S_1$)] is described by two triply degenerate molecular potentials α: $|w=1, \Lambda=0, \mu\rangle \equiv c^3\Sigma_g^+$ and $|w=-1, \Lambda=0, \mu\rangle \equiv a^3\Sigma_u^+$. The index $\mu=-1,0,1$ refers to the projection of the total spin on the molecular axis. The BO potential curves are known to spectroscopic accuracy [26,27].

The final channel β refers to the He($1\ ^1S$)+He($2\ ^3P$) interaction. The situation is more uncertain here and the potential energy curves are not known with sufficient accuracy [25]. The Hilbert space of the separated atoms has dimension $2\times(2S+1)\times(2L+1)=18$ and the total electronic angular momentum has values $j_\beta=0,1,2$. The number of basic vectors is the same in the molecular frame. Indeed, there are four molecular curves, two with threefold spin degeneracy and another two with sixfold (spin+Λ) degeneracy—they are

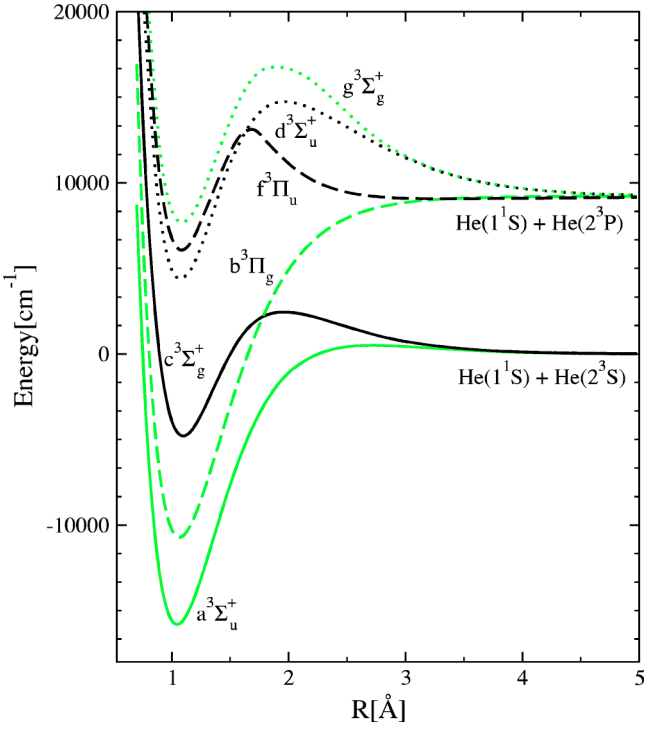

FIG. 3. (Color online) The relevant molecular potential energy curves for the pressure broadening and shift of He(^3S)-He(^3P) lines. The potential energy curves dissociating to He($1\ ^1S_0$) and He($2\ ^3P_j$) levels have been calculated in this work.

$$|w=1,\ \Lambda=0,\ \mu\rangle \equiv g^3\Sigma_g^+,$$

$$|w=-1,\ \Lambda=0,\ \mu\rangle \equiv d^3\Sigma_u^+,$$

$$|w=1,\ |\Lambda|=1,\ \mu\rangle \equiv b^3\Pi_g,$$

$$|w=-1,\ |\Lambda|=1,\ \mu\rangle \equiv f^3\Pi_u.$$

The BO potential energy curves correlating to the He($1\ ^1S_0$)-He($2\ ^3S_1$) ($a\ ^3\Sigma_u^+$ and $c\ ^3\Sigma_g^+$) have been constructed using rovibrational and differential scattering data and have been shown to be highly accurate in determining a number of scattering properties at low temperatures [26,27]. Yarkony [28] calculated the $b\ ^3\Pi_g$ symmetry correlating to He($1\ ^1S_0$) and He($2\ ^3P_j$) atomic levels. The only other *ab initio* calculation of the BO potential energies is due to Apkarian and Eloranta [25], who used an internally contracted multireference configuration interaction method to obtain the potential energies for other symmetries. The potentials were obtained for nuclear separations up to 4 Å. The difference between the rovibrational transition frequencies calculated using these potentials and the experimental [29] values was usually 200 cm^{-1} or more. To calculate the collisional broadening and shift in helium discharge, we need accurate molecular potentials over a sufficiently broad range of internuclear distances. To our knowledge, no attempt in calculating the long-range dispersion coefficients exists in the literature.

We calculated the excited He_2^* potentials over a range of nuclear separations. To this end, we applied a configuration interaction valence bond (CIVB) method, proven to be a reliable tool for finding ground and excited potentials of various dimers [32]. A complete description of the method used to calculate the He_2 excited-state potentials and the dispersion coefficients will be presented elsewhere [30]. The calculated potential energies are shown in Fig. 3.

The *ab initio* points are interpolated by cubic splines and extrapolated in a smooth fashion onto the long-range region using the van der Waals values $C_6=22.35$ a.u. and $C_8=1137$ a.u. for all molecular states in the final channel. We used a semiempirical technique—i.e., a mix of calculated and measured oscillator strengths—to compute the C_6 coefficient for the $He(1\ ^1S_0)+He(2\ ^3P_j)$ interaction [30,31] and the value of C_8 was obtained from a best fit to Yarkony's data for the $b\ ^3\Pi_g$ potential. The dynamic polarizability for the $He(1\ ^1S_0)$ is calculated by diagonalizing the two-electron Hamiltonian in a box and for the $He(2\ ^3P_j)$ is obtained from published oscillator strengths and photoionization cross section. In order to obtain a good asymptotic match of our numerical $f\ ^3\Pi_u$ potential energy to the dispersion potential, we needed to raise the energies throughout R by about 5 cm^{-1}. This procedure helped in improving agreement with the observed $f\ ^3\Pi_u \rightarrow c\ ^3\Sigma_g^+$ frequencies; see below. We chose the matching point between long and intermediate ranges at 6.0 Å for the $b\ ^3\Pi_g$ potential, at 10.5 Å for the $f\ ^3\Pi_u$ potential, and at 5.0 Å for the $d\ ^3\Sigma_u$ and $g\ ^3\Sigma_g$ potentials.

The $f\ ^3\Pi_u$ molecular state in Ref. [25] suffers from two deficiencies: the rovibrational transition frequencies in the $f\ ^3\Pi_u \rightarrow c\ ^3\Sigma_g^+$ bands are different from the measured values by more than 200 cm^{-1}, and the asymptotic well is too deep for a van der Waals potential. The $f\ ^3\Pi_u$ potential curve is critical in the evaluation of the pressure broadened and shift parameters because of the fact that it contains a long-range van der Waals well that dramatically influences the collisional phase shift. The quality of our *ab initio* curve is assessed by calculating the rovibrational energy levels and comparing the rovibrational transitions in the $f\ ^3\Pi_u \rightarrow c\ ^3\Sigma_g^+$ bands with available experimental data [29] and by ensuring that the long-range form of the potential asymptotically converges to the correct dispersion form. The differences in the rovibrational frequencies are, in general, less than 1%, but for the ends of the Q bands the error can be as high as 1.5%.

B. Broadening and shift of metastable helium spectral lines

For the collision between ground and metastable helium atoms, $j_\alpha=1$ and $j_\beta=0$, 1, 2 will be simply referred as j. All the matrix elements are diagonal in the total angular momentum J and its SF frame projection M.

The frame-transformed reduced matrix elements (8) for the initial channel α are

$$\langle 1\ell|w\mu\rangle = g^{(\alpha)}(w,\ell)\sqrt{\frac{2\ell+1}{2J+1}}C^{JM}_{\ell 01\mu}, \tag{10}$$

where the symmetry factor g is defined by

$$g^{(\alpha)}(w,\ell)\equiv\frac{1+w(-1)^\ell}{2}=\begin{cases}1 & \text{for even } \ell,\\ 0 & \text{for odd } \ell.\end{cases}$$

The corresponding factor in the final channel is

$$g^{(\beta)}(w,\ell)\equiv\frac{1-w(-1)^\ell}{2}=\begin{cases}0 & \text{for even } \ell,\\ 1 & \text{for odd } \ell,\end{cases}$$

and the transformation matrix elements (8) are given by

$$\langle j\ell|w\Lambda\mu\rangle = g^{(\beta)}(w,\ell)\sqrt{\frac{2\ell+1}{2J+1}}C^{JM}_{\ell 0j\Omega}C^{j\Omega}_{1\Lambda 1\mu}. \tag{11}$$

Equations (10) and (11) can be used to transform between the SF and BF frames, as in Eq. (9).

By combining Eqs. (9) and (10), the scattering matrix elements in the initial channel have the simple forms

$$\begin{aligned}S^{(J)}_{1\ell\rightarrow 1\ell'} &= \delta_{\ell\ell'}\sum_w g^{(\alpha)}(w,\ell)e^{2i\eta^{(J)}_w}\\ &= \delta_{\ell\ell'}\begin{cases}e^{2i\eta^{(J)}_c} & \text{for even } \ell,\\ e^{2i\eta^{(J)}_a} & \text{for odd } \ell.\end{cases}\end{aligned} \tag{12}$$

The expression for the scattering matrix elements in the final channel is more complicated:

$$\begin{aligned}S^{(J)}_{j\ell\rightarrow j'\ell'} &= \sum_{w\Lambda} g^{(\beta)}(w,\ell)g^{(\beta)}(w,\ell')\frac{\sqrt{(2\ell+1)(2\ell'+1)}}{2J+1}\\ &\times e^{2i\eta^{(J)}_{w|\Lambda|}}\sum_\mu C^{JM}_{\ell 0j\Omega}C^{j\Omega}_{1\Lambda 1\mu}C^{JM}_{\ell' 0j'\Omega}C^{j'\Omega}_{1\Lambda 1\mu}.\end{aligned} \tag{13}$$

The complex broadening and shift cross section in Eq. (5), labeled only by the total atomic angular momentum j in the final state, is then

$$\begin{aligned}\sigma_j = \frac{\pi}{k^2}\sum_{J_\alpha J_\beta \ell}(2J_\alpha+1)(2J_\beta+1)\begin{Bmatrix}J_\beta & J_\alpha & 1\\ 1 & j_\beta & \ell\end{Bmatrix}^2\\ \times\left(1-\sum_{ww'\Lambda}e^{2i(\eta^{(J_\alpha)}_w-\eta^{(J_\beta)}_{w'|\Lambda|})}g^{(\alpha)}(w,\ell)\right.\\ \left.\times g^{(\beta)}(w',\ell)A^{j\ell J_\beta}_\Lambda\right),\end{aligned} \tag{14}$$

where the quantity A is shorthand notation for

$$A^{j\ell J}_\Lambda = \frac{2\ell+1}{2J+1}\sum_\mu (C^{JM}_{\ell 0j\Omega})^2(C^{j\Omega}_{1\Lambda 1\mu})^2.$$

TABLE I. The kinematic mixing coefficients $B^{jJJ_\beta}_{ww'\Lambda}$ in Eq. (17).

$\eta_w^{(J_\alpha)} - \eta_{w'\|\Lambda\|}^{(J_\beta)}$	c-d	c-f	a-g	a-b
		$j=0$, even J		
$(J,J-1)$	0	0	$\frac{1}{9}$	$\frac{2}{9}$
(J,J)	$\frac{1}{9}$	$\frac{2}{9}$	0	0
$(J,J+1)$	0	0	$\frac{1}{9}$	$\frac{2}{9}$
		$j=0$, odd J		
$(J,J-1)$	$\frac{1}{9}$	$\frac{2}{9}$	0	0
(J,J)	0	0	$\frac{1}{9}$	$\frac{2}{9}$
$(J,J+1)$	$\frac{1}{9}$	$\frac{2}{9}$	0	0
		$j=1$, even J		
$(J,J-1)$	$\frac{(J-1)(J+1)}{12J(2J+1)}$	$\frac{(J+1)(3J-1)}{12J(2J+1)}$	$\frac{(J-1)}{12J}$	$\frac{(J-1)}{12J}$
(J,J)	$\frac{1}{112J(J+1)}$	$\frac{1}{112J(J+1)}$	$\frac{J^2+J+1}{12J(J+1)}$	$\frac{3J^2+3J+1}{12J(J+1)}$
$(J,J+1)$	$\frac{J(J+2)}{12(J+1)(2J+1)}$	$\frac{J(3J+4)}{12(J+1)(2J+1)}$	$\frac{J+2}{12(J+1)}$	$\frac{J+2}{12(J+1)}$
		$j=1$, odd J		
$(J,J-1)$	$\frac{(J-1)}{12J}$	$\frac{(J-1)}{12J}$	$\frac{(J-1)(J+1)}{12J(2J+1)}$	$\frac{(J+1)(3J-1)}{12J(2J+1)}$
(J,J)	$\frac{J^2+J+1}{12J(J+1)}$	$\frac{3J^2+3J+1}{12J(J+1)}$	$\frac{1}{112J(J+1)}$	$\frac{1}{112J(J+1)}$
$(J,J+1)$	$\frac{J+2}{12(J+1)}$	$\frac{J+2}{12(J+1)}$	$\frac{J(J+2)}{12(J+1)(2J+1)}$	$\frac{J(3J+4)}{12(J+1)(2J+1)}$
		$j=2$, even J		
$(J,J-1)$	$\frac{(J-1)(J+1)}{20J(2J+1)}$	$\frac{3(J-1)^2}{20J(2J+1)}$	$\frac{38J^2-5J-9}{180J(2J+1)}$	$\frac{46J^2-61J+27}{180J(2J+1)}$
(J,J)	$\frac{4J^2+4J+9}{180J(J+1)}$	$\frac{20J^2+20J-27}{180J(J+1)}$	$\frac{J^2+J+1}{20J(J+1)}$	$\frac{3(J^2+J-1)}{20J(J+1)}$
$(J,J+1)$	$\frac{J(J+2)}{20(J+1)(2J+1)}$	$\frac{3(J+2)^2}{20(J+1)(2J+1)}$	$\frac{38J^2+81J+34}{180(J+1)(2J+1)}$	$\frac{46J^2+153J+134}{180(J+1)(2J+1)}$
		$j=2$, odd J		
$(J,J-1)$	$\frac{38J^2-5J-9}{180J(2J+1)}$	$\frac{46J^2-61J+27}{180J(2J+1)}$	$\frac{(J-1)(J+1)}{20J(2J+1)}$	$\frac{3(J-1)^2}{20J(2J+1)}$
(J,J)	$\frac{J^2+J+1}{20J(J+1)}$	$\frac{3(J^2+J-1)}{20J(J+1)}$	$\frac{4J^2+4J+9}{180J(J+1)}$	$\frac{20J^2+20J-27}{180J(J+1)}$
$(J,J+1)$	$\frac{38J^2+81J+34}{180(J+1)(2J+1)}$	$\frac{46J^2+153J+134}{180(J+1)(2J+1)}$	$\frac{J(J+2)}{20(J+1)(2J+1)}$	$\frac{3(J+2)^2}{20(J+1)(2J+1)}$

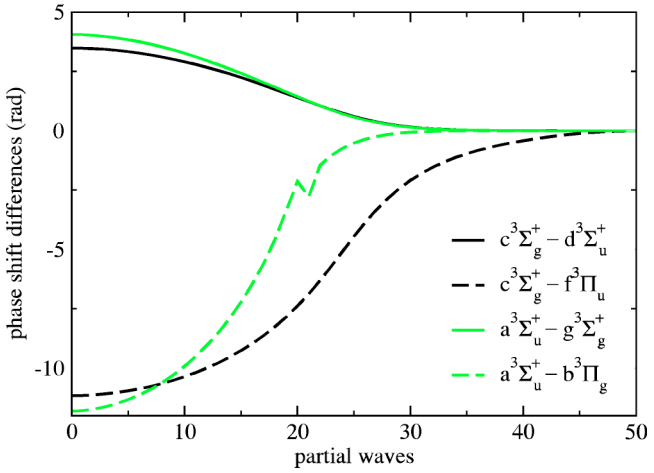

FIG. 4. (Color online) Differences relevant to the pressure broadening and shift of metastable helium lines, between phase shifts for the collisional energy of 211 cm^{-1} in both the initial and final channels.

It is not difficult to show that $\Sigma_\Lambda A_\Lambda^{j\ell J}=1$, which allows for writing the broadening-shift cross section in a more compact form

$$\sigma_j=\frac{\pi}{k^2}\sum_J (2J+1)\sum_{J_\beta w w' \Lambda} Z^{JJ_\beta}_{ww'\Lambda}(v)B^{jJJ_\beta}_{ww'\Lambda} \qquad (15)$$

that disentangles the energy-dependent part

$$Z^{JJ_\beta}_{ww'\Lambda}(v)=1-e^{2i(\eta_w^{(J_\alpha)}-\eta_{w'|\Lambda|}^{(J_\beta)})} \qquad (16)$$

from the kinematic part of the cross section:

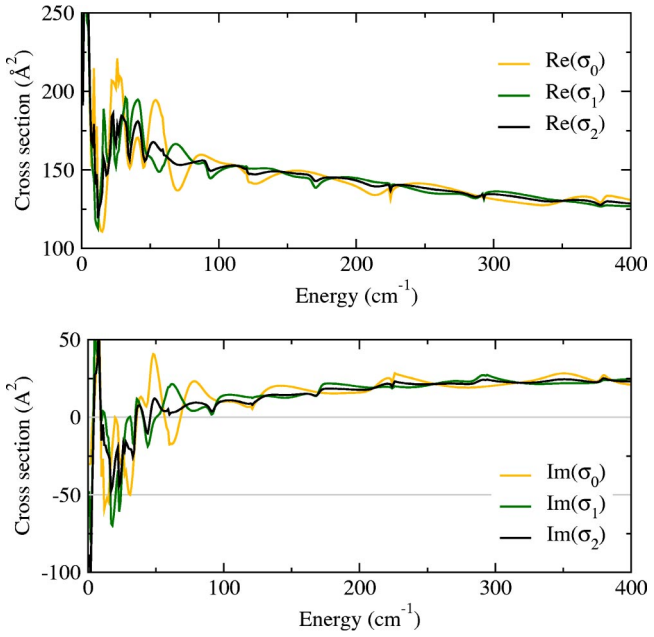

FIG. 5. (Color online) The real and imaginary parts of the broadening-shift cross section of metastable helium lines as a function of energy.

TABLE II. Pressure broadening and shift rates (in MHz/Torr) for metastable helium transition lines He($2\,^3S_1$)-He($2\,^3P_{j_\beta}$) perturbed by collisions with the ground-state helium atoms, in the 200–400 K temperature range.

	$j_\beta=0$		$j_\beta=1$		$j_\beta=2$	
T (K)	w/p	d/p	w/p	d/p	w/p	d/p
200	15.58	−2.03	15.61	−2.00	15.60	−1.93
210	15.11	−2.02	15.14	−2.00	15.13	−1.93
220	14.68	−2.01	14.71	−1.99	14.69	−1.93
230	14.27	−2.00	14.30	−1.98	14.29	−1.92
240	13.90	−1.99	13.92	−1.97	13.91	−1.92
250	13.54	−1.98	13.57	−1.96	13.56	−1.91
260	13.21	−1.96	13.23	−1.95	13.23	−1.91
270	12.89	−1.95	12.92	−1.94	12.91	−1.90
280	12.60	−1.93	12.62	−1.92	12.61	−1.89
290	12.32	−1.92	12.34	−1.91	12.33	−1.87
300	12.05	−1.91	12.07	−1.90	12.07	−1.86
310	11.79	−1.89	11.82	−1.88	11.81	−1.85
320	11.55	−1.88	11.57	−1.87	11.57	−1.84
330	11.32	−1.86	11.34	−1.85	11.34	−1.82
340	11.10	−1.84	11.12	−1.84	11.11	−1.81
350	10.88	−1.83	10.90	−1.82	10.90	−1.80
360	10.68	−1.81	10.70	−1.81	10.70	−1.78
370	10.48	−1.80	10.50	−1.79	10.50	−1.77
380	10.29	−1.78	10.31	−1.77	10.31	−1.75
390	10.10	−1.76	10.12	−1.76	10.12	−1.74
400	9.92	−1.75	9.94	−1.74	9.94	−1.72

$$B^{jJJ_\beta}_{ww'\Lambda}=\sum_\ell g^{(\alpha)}(w,\ell)g^{(\beta)}(w',\ell)\begin{Bmatrix} J_\beta J 1 \\ 1 j_\beta \ell \end{Bmatrix}^2 A_\Lambda^{j\ell J_\beta}. \qquad (17)$$

Coefficients B have nonzero values only when $ww'=-1$ and, therefore, the only possible $ww'\Lambda$ combinations are c-d, c-f, a-g, and a-b; see Fig. 3 for notation. The total angular momentum in the final channel can only have three values $J_\beta=J-1,J,J+1$. The mixing coefficients do not depend on the details of the interaction and embody both the frame transformation and the kinematics of the photon-diatom angular momentum coupling. These coefficients, listed in Table I for all possible combinations, reduce to simple expressions and could be use for independent calculations of the shift-broadening cross section.

The relevant elastic phase shift differences for several partial waves populated at a collision energy of 211 cm^{-1} are shown in Fig. 4. The largest differences are for the a-b and c-f dipole-allowed transitions.

The real and imaginary parts of the broadening-shift cross section in Eq. (5) for different He($2\,^3P_j$) levels are shown in Fig. 5. For energies larger than 200 cm^{-1}, the broadening and shift cross section becomes j independent. This is to be expected, as at high collision energies the fine-structure splitting, which is less than 1 cm^{-1}, will not appreciably affect the scattering in the molecular potential wells.

Table II lists the main results of this work: namely, the pressure broadening and shift parameters from Eq. (4) in

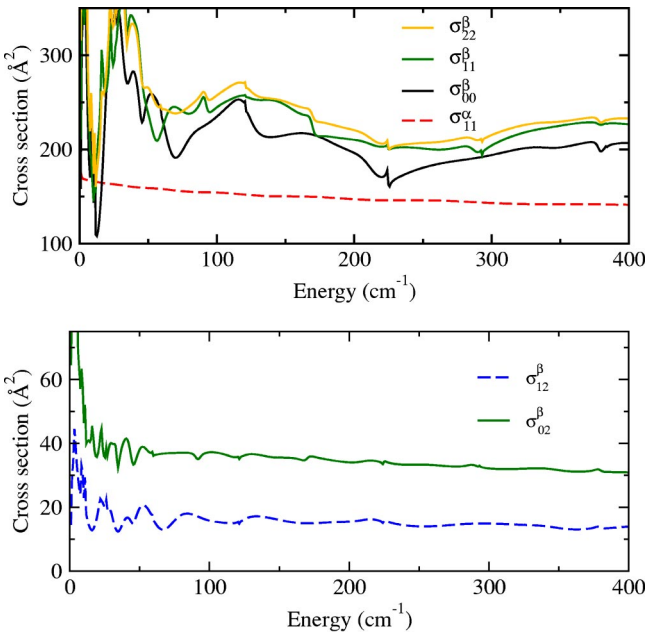

FIG. 6. (Color online) Cross sections for j-specific and j-changing collisions between normal and metastable helium atoms.

units of MHz/Torr. At the temperatures of the experiment, roughly 310 K, there is little difference between the results for different j levels. It should be noted that the natural linewidth $\Gamma/2=0.8$ MHz should be added to the collisional broadening parameter w for comparison with the experimental results. Collisional interactions thus produce significant broadening and shift of the spectral lines in collisions of He($1\ ^1S_0$) and He($2\ ^3S_1$) and He($2\ ^3P_j$) atoms. Our predictions are in good agreement with the preliminary analysis of the experiment [21].

C. Scattering cross sections

The cross sections for elastic ($j'=j$) and j-changing collisions between ground-state He($1\ ^1S_0$) and metastable He($2\ ^3S_1$) and He($2\ ^3P_j$) atoms are readily available once the S-matrix elements in the initial (12) and final (13) channels are obtained. In the elastic approximation, these cross sections are, in general, given by

$$\sigma_{j'j}=\frac{\pi}{k^2}\sum_{J,\ell,\ell'}\frac{2J+1}{2j+1}|\delta_{j'j}\delta_{\ell'\ell}-S^{(J)}_{j'\ell';j\ell}|^2.$$

There are no j-changing collisions in the initial channel and the elastic cross section follows from Eq. (12) and has the simple expression

$$\sigma^{\alpha}_{11}=\frac{4\pi}{3k^2}\left[\sum_J (2J+1)(2\sin^2\eta^{(J)}_p+\sin^2\eta^{(J)}_q)\right],$$

where the subscripts (p,q) refer to the molecular potentials (a,c) for even J values and to the molecular potentials (c,a) for odd J values, respectively.

Figures 6 illustrate the j-specific and j-changing cross sections as a function of collision energy. The elastic cross sections are 4–5 times larger than the j-changing cross sections, with the $j=2\rightarrow j'=1$ cross section twice as large as the $j=2\rightarrow j'=0$ cross section. The cross section for $j=1\rightarrow j'=0$ is zero because one of the Clebsch-Gordan coefficients (C^{10}_{1010}) in Eq. (13) vanishes. The three elastic cross sections in the final channel are 50%–60% larger than the initial channel cross section.

IV. CONCLUSIONS

Using an improved *ab initio* set of helium ground-metastable interaction potentials, line broadening and shift parameters have been obtained in the impulse approximation for the three He($2\ ^3S_1$)-He($2\ ^3P_j$)($j=0,1,2$) fine-structure transitions perturbed by collisions with He($1\ ^1S_0$) atoms. Short-range Born-Oppenheimer potentials are found by using the multiconfigurational valence bond method. The van der Waals coefficients for the excited-state interaction have been semiempirically calculated. The pressure coefficients show a weak dependence on the total angular momentum quantum number of the final states over the range of temperatures considered (200–400 K), as can be expected from the fact that the collision energies are much greater than the fine-structure splitting between the He(^3P) energy levels.

The j-changing and elastic scattering cross sections of the ground-state atom He($1\ ^1S_0$) and the metastable He($2\ ^3S_1$) and He($2\ ^3P_j$) atoms are also calculated. The cross sections for collisions which change the fine structure in He($2\ ^3P_j$) atoms are 4–5 times smaller than the cross sections for elastic collisions.

ACKNOWLEDGMENTS

This work is supported by NSF through a grant for the Institute of Theoretical Atomic, Molecular and Optical Physics (ITAMP) at Harvard University and Smithsonian Astrophysical Observatory. We thank T. Roach for discussions in the early phase of this work. We are also indebted to T. Zelevinsky and G. Gabrielse for access to measurements and numerous discussions.

APPENDIX

The scattering matrix elements are defined in a basis of separated atoms in the SF frame,

$$\Psi^{JM}_{j_1j_2j\ell}(\hat{\mathbf{R}},\mathbf{r})=\sum_{\substack{m,n\\ m_1,m_2}} C^{JM}_{\ell njm}Y_{\ell n}(\hat{\mathbf{R}})C^{jm}_{j_1m_1j_2m_2}\times\varphi_{j_1m_1}(\mathbf{r}_{iA})\varphi_{j_2m_2}(\mathbf{r}_{jB}),$$

where $\hat{\mathbf{R}}$ is the direction along the internuclear axis, $\mathbf{R}=\mathbf{r}_A-\mathbf{r}_B$, $\mathbf{r}$ stands for the full set electronic coordinates $(\mathbf{r}_1,\mathbf{r}_2,\mathbf{r}_3,\mathbf{r}_4)$, and φ_{jm} are the wave functions for electrons 1 and 2 bound to the nucleus A and electrons 3 and 4 bound to the nucleus B, with relative coordinates $\mathbf{r}_{iA}=\mathbf{r}_i-\mathbf{r}_A$ for $i=1,2$ and $\mathbf{r}_{jB}=\mathbf{r}_j-\mathbf{r}_B$ for $j=3,4$. These wave functions are eigenstates of the total angular momentum operator and its projection on the SF z axis with eigenvalues J and M. Inver-

sion of the coordinate system and nuclear and electronic exchange together with angular momentum form the complete set of commuting observables.

The properly normalized electronic wave function at $R \to \infty$, symmetric with respect to the electron exchange, is

$$\varphi_{jm}^{(j_1 j_2)}(\mathbf{r}) = \mathcal{A} \sum_{m_1 m_2} C^{jm}_{j_1 m_1 j_2 m_2} \varphi_{j_1 m_1}(\mathbf{r}_{iA}) \varphi_{j_2 m_2}(\mathbf{r}_{jB}),$$

where $\mathcal{A}$ is electronic antisymmetrization operator.

The coordinate inversion operator is described by

$$\mathcal{I} \equiv (\mathbf{r}_{iA} \to -\mathbf{r}_{iA}, \mathbf{r}_{jB} \to -\mathbf{r}_{jB}, \mathbf{R} \to -\mathbf{R}),$$

whose action on SF wave functions is

$$\mathcal{I} \Psi^{JM}_{j_1 j_2 j \ell} = w_1 w_2 (-1)^{\ell} \Psi^{JM}_{j_1 j_2 j \ell},$$

where $w_{1,2}$ are the corresponding atomic parities.

The operator $\mathcal{P}_{AB}$ exchanges the two nuclei,

$$\mathcal{P}_{AB} \equiv (\mathbf{r}_{iA} \to \mathbf{r}_{iB}, \mathbf{r}_{jB} \to \mathbf{r}_{jA}, \mathbf{R} \to -\mathbf{R}),$$

but it is convenient to use instead the electronic inversion operator $\mathcal{I}_e = \mathcal{I}\mathcal{P}_{AB}$, defined by

$$\mathcal{I}_e \equiv (\mathbf{r}_{iA} \to -\mathbf{r}_{iB}, \mathbf{r}_{jB} \to -\mathbf{r}_{jA}, \mathbf{R} \to \mathbf{R}),$$

as it acts only on the electronic coordinates. Because $\mathcal{I}_e$ commutes with $\mathcal{A}$, then

$$\begin{aligned} \mathcal{I}_e \varphi_{jm}^{(j_1 j_2)}(\mathbf{r}) &= \mathcal{A} \sum_{m_1 m_2} C^{jm}_{j_1 m_1 j_2 m_2} w_1 \varphi_{j_1 m_1}(\mathbf{r}_{iB}) w_2 \varphi_{j_2 m_2}(\mathbf{r}_{jA}) \\ &= w_1 w_2 \mathcal{A} \sum_{m_1 m_2} C^{jm}_{j_1 m_1 j_2 m_2} \varphi_{j_1 m_1}(\mathbf{r}_{jB}) \varphi_{j_2 m_2}(\mathbf{r}_{iA}) \\ &= w_1 w_2 (-1)^{N + j_1 + j_2 - j} \varphi_{jm}^{(j_2 j_1)}(\mathbf{r}), \end{aligned}$$

where $N=2$ is the number of electrons in a He atom. This factor comes from the fact that it takes exactly two permutations to transform indices i to j.

The operator $\mathcal{I}_e$ can also be interpreted as the inversion of electronic coordinates through the geometric center of the nuclei. If $\mathbf{r}_C = (\mathbf{r}_A + \mathbf{r}_B)/2$, then $\mathbf{r}_i = \mathbf{r}_C + \mathbf{r}_{iC}$, where $\mathbf{r}_{iC}$ is the position vector of electron i relative to center C. On inversion through the center, $\mathbf{r}_{iC} \to -\mathbf{r}_{iC}$, and therefore $\mathbf{r}_i \to 2\mathbf{r}_C - \mathbf{r}_i = \mathbf{r}_A + \mathbf{r}_B - \mathbf{r}_i$. The relative coordinate of electron i with respect to nucleus A transforms as $\mathbf{r}_{iA} \to \mathbf{r}_B - \mathbf{r}_i = -\mathbf{r}_{iB}$ and, similarly, $\mathbf{r}_{jB} \to -\mathbf{r}_{jA}$. Since nuclear coordinates are not affected by this transformation, $\mathcal{I}_e$ is indeed the inversion operator for the electronic coordinates through the midpoint on the nuclear axis.

The SF wave function

$$\Psi^{JM}_{(j_1 j_2) j \ell}(\hat{R}, \mathbf{r}) = \frac{1}{\sqrt{2}} (1 + p_e \mathcal{I}_e) \sum_{m,n} C^{JM}_{\ell n j m} Y_{\ell n}(\hat{R}) \varphi_{jm}^{(j_1 j_2)}(\mathbf{r})$$

is an eigenfunction of $\mathcal{I}$, $\mathcal{I}_e$, and $\mathcal{P}_{ij}$, and $p_e = p p_{AB} = w_1 w_2 (-1)^{\ell} p_{AB}$. Finally, the symmetrized SF wave function

$$\begin{aligned} \Psi^{JM}_{(j_1 j_2) j \ell}(\hat{R}, \mathbf{r}) = \frac{1}{\sqrt{2}} \sum_{m,n} C^{JM}_{\ell n j m} Y_{\ell n}(\hat{R}) [& \varphi_{jm}^{(j_1 j_2)}(\mathbf{r}) \\ & + p_{AB} (-1)^{j_1 + j_2 - j + \ell} \varphi_{jm}^{(j_2 j_1)}(\mathbf{r})] \end{aligned} \quad \text{(A1)}$$

describes the system of two separated atoms with total parity $p = w_1 w_2 (-1)^{\ell}$ and electronic inversion parity $p_e = w_1 w_2 (-1)^{\ell} p_{AB}$.

A more convenient basis for evaluating the scattering matrix is the BF basis, composed of Born-Oppenheimer eigenfunctions evaluated at a fixed R in the BF frame. The nuclear wave function is that of a symmetric top, while the electronic coordinates denoted as $\mathbf{r}'$ have components with respect to the moving reference frame. The definition of molecular basis is

$$\Psi^{JM}_{cw\Lambda\mu}(\hat{\mathbf{R}}; \mathbf{r}) = \sqrt{\frac{2J+1}{4\pi}} D^{(J)}_{M\Omega}{}^*(\phi, \theta, 0) \lim_{R \to \infty} \varphi_{cw\Lambda\mu}(R; \mathbf{r}'),$$

where c stands for the spectroscopic notation of a level and the rest are defined just after Eq. (7). In the limit of large nuclear separation, the BF electronic wave functions are obtained by symmetrizing in the coupled-spin representation, with a given projection of the total orbital angular momentum on the z axis of the BF frame, as

$$\varphi_{\Lambda\mu}^{(\Lambda_1 \Lambda_2)}(\mathbf{r}') = \mathcal{A} \sum_{L_1 L_2} C^{L\Lambda}_{L_1 \Lambda_1 L_2 \Lambda_2} \varphi_{L_1 \Lambda_1}(\mathbf{r}'_{i_A}) \varphi_{L_1 \Lambda_1}(\mathbf{r}'_{j_B}) \chi^S_{\mu}.$$

The gerade-ungerade character of the molecular function, eigenvalues of the electronic inversion operator $\mathcal{I}_e$, is preserved when $R \to \infty$—the action of this operator—is the same in both SF and BF frames.

The properly symmetrized molecular wave functions are therefore

$$\begin{aligned} \Psi^{JM}_{w\Lambda\mu}(\hat{\mathbf{R}}; \mathbf{r}) = \sqrt{\frac{2J+1}{8\pi}} D^{(J)}_{M\Omega}{}^*(\phi, \theta, 0) [& \varphi_{\Lambda\mu}^{(\Lambda_1 \Lambda_2)}(\mathbf{r}') \\ & + w w_1 w_2 \varphi_{\Lambda\mu}^{(\Lambda_2 \Lambda_1)}(\mathbf{r}')]. \end{aligned} \quad \text{(A2)}$$

[1] A. Döhrn *et al.*, Phys. Rev. E **53**, 6389 (1996).

[2] S.I. Knorsky *et al.*, Phys. Rev. B **50**, 6296 (1994).

[3] J. Cooper, Rev. Mod. Phys. **39**, 167 (1967); K. Burnett *et al.* Phys. Rev. A **22**, 2005 (1980).

[4] P.S. Julienne and F.H. Mies, Phys. Rev. A **34**, 3792 (1986).

[5] J. Szudy and W.E. Baylis, Phys. Rep. **266**, 127 (1996).

[6] N. Allard and J. Kielkopf, Rev. Mod. Phys. **54**, 1103 (1982).

[7] M. Baranger, Phys. Rev. **111**, 481 (1958); **112**, 855 (1958).

[8] H.G. Kuhn, Proc. R. Soc. London, Ser. A **158**, 212 (1937).
[9] P.R. Berman, Phys. Rev. A **13**, 2191 (1976).
[10] F. Minardi, G. Bianchini, P. Cancio Pastor, G. Giusfredi, F.S. Pavone, and M. Inguscio, Phys. Rev. Lett. **82**, 1112 (1999).
[11] C.H. Storry, M.C. George, and E.A. Hessels, Phys. Rev. Lett. **84**, 3274 (2000).
[12] M.C. George, L.D. Lombardi, and E.A. Hessels, Phys. Rev. Lett. **87**, 173002 (2001).
[13] T. Zelevinsky and G. Gabrielse, in Proceedings of the DAMOP Meeting [Bull. Am. Phys. Soc. **48**, 58 2003].
[14] U. Fano, Phys. Rev. A **2**, 353 (1972).
[15] A.M. Arthurs and A. Dalgarno, Proc. R. Soc. London, Ser. A **256**, 540 (1960).
[16] S.J. Singer, K.F. Freed, and Y.B. Band, J. Chem. Phys. **79**, 6060 (1983).
[17] R.T. Pack and J.O. Hirschfelder, J. Chem. Phys. **49**, 4009 (1968).
[18] R.H.G. Reid and R.F. Rankin, J. Phys. B **11**, 55 (1978).
[19] P.J. Leo, G. Peach, and I.B. Whittingham, J. Phys. B **28**, 591 (1995).
[20] R.V. Krems and A. Dalgarno, Phys. Rev. A **66**, 012702 (2002).
[21] T. Zelevinsky and G. Gabrielse (unpublished).
[22] U. Fano, Phys. Rev. **131**, 259 (1963).
[23] G. Peach, Comments At. Mol. Phys. **11**, 101 (1982).
[24] K.S. Barnes and G. Peach, J. Phys. B **3**, 350 (1970).
[25] A. Apkarian and J.S. Eloranta, J. Chem. Phys. **115**, 752 (2001).
[26] R.M. Jordan, H.R. Saddiqui, and P.E. Siska, J. Chem. Phys. **84**, 6719 (1986).
[27] D. Vrinceanu and H.R. Sadeghpour, Phys. Rev. A **65**, 062712 (2002).
[28] D.R. Yarkony, J. Chem. Phys. **90**, 164 (1989).
[29] M.L. Ginter and R. Battino, J. Chem. Phys. **52**, 469 (1970); M.L. Ginter, *ibid.* **42**, 61 (1965).
[30] S. Kotochigova, D. Vrinceanu, and H.R. Sadeghpour (unpublished).
[31] NIST Atomic Spectra Database, http://physics.nist.gov/cgi-bin/AtData/
[32] S. Kotochigova, E. Tiesinga, and I. Tupitsyn, Phys. Rev. A **61**, 042712 (2000); in *New Trends in Quantum Systems in Chemistry and Physics*, edited by J. Maruani, C. Minot, R. McWeeny, Y.G. Sweyers, and S. Wilson (Kluwer Academic, Dordrecht, 2001), Vol. 1, p. 219; E. Tiesinga, S. Kotochigova, and P.S. Julienne, Phys. Rev. A **65**, 042722 (2002); S. Kotochigova, E. Tiesinga, and P.S. Julienne, *ibid.* **68**, 022501 (2003).